Carbohydrate Polymers 325 (2024) 121561

Contents lists available at ScienceDirect

Carbohydrate Polymers

journal homepage: www.elsevier.com/locate/carbpol

Chitin-based pulps: Structure-property relationships and environmental sustainability

Luiz G. Greca [a,b,*,1], Ainara Azpiazu [a,c,1], Guillermo Reyes [a], Orlando J. Rojas [a,d,*], Blaise L. Tardy [e,f,g], Erlantz Lizundia [c,h,**]

[a] Department of Bioproducts and Biosystems, School of Chemical Engineering, Aalto University, P.O. Box 16300, FI-00076 Aalto, Finland
[b] Swiss Federal Laboratories for Materials Science and Technology (EMPA), Cellulose & Wood Materials Laboratory, Dübendorf, 8600, Switzerland
[c] Life Cycle Thinking Group, Department of Graphic Design and Engineering Projects, University of the Basque Country (UPV/EHU), Plaza Ingeniero Torres Quevedo 1, 48013 Bilbao, Biscay, Spain
[d] Bioproducts Institute, Department of Chemical and Biological Engineering, Department of Chemistry, and Department of Wood Science, University of British Columbia, 2360 East Mall, Vancouver, BC V6T 1Z4, Canada
[e] Department of Chemical Engineering, Khalifa University, United Arab Emirates
[f] Center for Membrane and Advanced Water Technology, Khalifa University, Abu Dhabi, United Arab Emirates
[g] Research and Innovation Center on CO_2 and Hydrogen, Khalifa University, Abu Dhabi, United Arab Emirates
[h] BCMaterials, Basque Center for Materials, Applications and Nanostructures, Edif. Martina Casiano, Pl. 3 Parque Científico UPV/EHU Barrio Sarriena, 48940 Leioa, Biscay, Spain

ARTICLE INFO

Keywords:
Chitin
Pulp
Green chemistry
Bioeconomy
Life cycle assessment
Environmental impact

ABSTRACT

The deconstruction and valorization of chitinous biomass from crustaceans is a promising route for sustainable bioproduct development alternative to petroleum-based materials. However, chitin nanocrystal and chitin nanofibril isolation from crustacean shells is often subjected to extensive processing, compromising their environmental and cost sustainability. To address the sustainability challenge that chitin valorization presents, herein we introduce a mild fibrillation route to generate "chitin pulp"; where a careful control of the macro- and microfibrillated chitin with protein and mineral components yields tailored properties. Films produced from protein-rich chitin pulp showed ultimate strength of up to 93 ± 7 MPa. The surface energy and wetting behavior, going from hydrophilic to nearly-hydrophobic, could be tailored as a function of pulp composition. Life cycle assessment of the protein-rich chitin pulps demonstrated that the global warming potential of chitin pulp is reduced by 2 to 3 times when compared to chitin nanocrystals. Overall, this work presents a new and potentially scalable route for the generation of chitin-based materials having a reduced environmental footprint compared to nanochitins and chitosan, thus opening a new route for the valorization of chitin beyond nanochitin for the development of environmentally and economically sustainable materials.

1. Introduction

Chitin, one of the major structural components in many living organisms, such as arthropods and fungi, is structurally similar to cellulose, although containing *N*-acetylglucosamine units over the β-(1 → 4)-linked D-glucose units from cellulose (Lizundia, Nguyen, Winnick, & MacLachlan, 2021). From the first wave of research on valorization of chitin, starting nearly 50 years ago, only chitosan has fully emerged as a viable chitin-derived product, with applications relying on its antibacterial properties and biocompatibility (Bai et al., 2022). More recently, a deconstructed native version of chitin fibrils, namely nanochitin, has been explored (Bai et al., 2022; Rinaudo, 2006). Nanochitin possesses remarkable mechanical properties, enabling natural dermal amours that resist large mechanical stresses (Zimmermann et al., 2013), and offers

* Corresponding authors at: Department of Bioproducts and Biosystems, School of Chemical Engineering, Aalto University, P.O. Box 16300, FI-00076 Aalto, Finland.
** Correspondence to: E. Lizundia, Life Cycle Thinking Group, Department of Graphic Design and Engineering Projects, University of the Basque Country (UPV/EHU), Plaza Ingeniero Torres Quevedo 1, 48013 Bilbao, Biscay, Spain.
E-mail addresses: luiz.greca@empa.ch (L.G. Greca), orlando.rojas@ubc.ca (O.J. Rojas), erlantz.liizundia@ehu.eus (E. Lizundia).
[1] These authors contributed equally.

https://doi.org/10.1016/j.carbpol.2023.121561
Received 28 July 2023; Received in revised form 13 October 2023; Accepted 2 November 2023
Available online 9 November 2023

potentially suitable optical properties for biomimicry (Lizundia et al., 2021). Furthermore, nanochitin presents a structure closer to that of naturally observed chitin, which can benefit from supramolecular interactions with other natural polymers such as proteins (Greca et al., 2021). These outstanding properties have resulted in notable efforts to extract nanochitin and implement this material into high-performance applications, including adhesives (Greca et al., 2021), battery separators and electrolytes (Kim et al., 2017; Ruiz, Michel, Niederberger, & Lizundia, 2023) enantioselective adsorption (Nguyen et al., 2019), optical sensing (Nguyen & Maclachlan, 2014) or mechanical reinforcement (Liu, Peng, Luo, & Zhou, 2015). The replacement of petroleum-based materials by chitin and its derivatives is a promising route for sustainable bioproduct development alternative to petroleum-based materials, circumventing current primary raw material scarcity (Seddon et al., 2020), reducing our global footprint (Cabernard, Pfister, Oberschelp, & Hellweg, 2022), and preventing the accumulation of plastic waste in terrestrial, river or marine ecosystems (Lebreton & Andrady, 2019).

The extensive purification and processing steps often required to generate nanochitin from crustacean biomass remains as one of the biggest challenges for its industrial viability. In crustacean shells, one of the most common chitin sources, chitin coexists with proteins and $CaCO_3$, which conventionally demands extraction approaches that require strong acid hydrolysis and/or chemical oxidation steps to demineralize and deproteinize the chitin. Furthermore, extensive mechanical processing and washing steps are, respectively, required to fibrillate and further purify the nanochitin (Bai et al., 2022). Besides the lack of cost-efficiency to be commercially viable, large environmental burdens originate from such use of strong inorganic acid/bases, energy intensive processes, and large volumes of generated wastewater.

These issues highlight the paramount need for milder and efficient processes that meets the material performance standards and minimal requirements for the manufacture of sustainable materials, *e.g.* those in packaging (Tardy et al., 2023). Several recent efforts have advanced the purification of varied forms of chitin from crustacean shells and other wastes, where mechanochemistry (Hajiali et al., 2022), and solvent-free processing (Jin et al., 2022), represent promising environmentally sustainable routes. Despite of such advancements, however, large scale industrial implementation in the short- and near-term may only be possible through the use of less processed forms of chitin, *i.e.* macro- and micro-scaled fibers, analogous to what is observed for cellulose (Li et al., 2021). Therefore, there is a need to rethink the need for extensive nanofibrilation and purification of chitinous materials, where the production of raw chitin pulp – more closely associated to natural fibers –would involve noteworthy economic and environmental cost reduction, while potentially keeping some of the outstanding properties of nanochitin (Chen et al., 2022; Shamshina, Barber, Gurau, Griggs, & Rogers, 2016).

In this work, we investigate the minimal processing of chitinous biomass into chitin-based pulps, and discuss the opportunities that may arise when preserving proteins, minerals, or both, from the original raw material. As summarized in Fig. 1, chitin pulp can be obtained from raw ocean waste; in this discussion, based on shrimp residues as a case study. We explore the effect processing routes ranging from mild to more severe processes that include individual or combined steps of ball milling, demineralization, and deproteinization, and evaluate the structural, wetting, and mechanical properties of films produced from the resulting chitin pulps. The obtained materials range from macro- to nano-structured, as a function of process severity. In spite of the *a priori* environmental benefits originated from chitin pulp production, it is also essential to provide unambiguous and accurate metrics that account for the related environmental impacts. Therefore, we utilize the life cycle assessment (LCA) methodology, following a standardized approach based on ISO 14040 and ISO 14044 standards, to quantify the environmental impacts (Laurent et al., 2020). Importantly, LCA enables the quantification of the greenhouse gas emissions associated with chitin-pulp production, especially relevant if industry targets a 45 % CO_2 emission reduction by 2030 (European Commission, n.d.). LCA also provides environmental metrics regarding eutrophication, acidification,

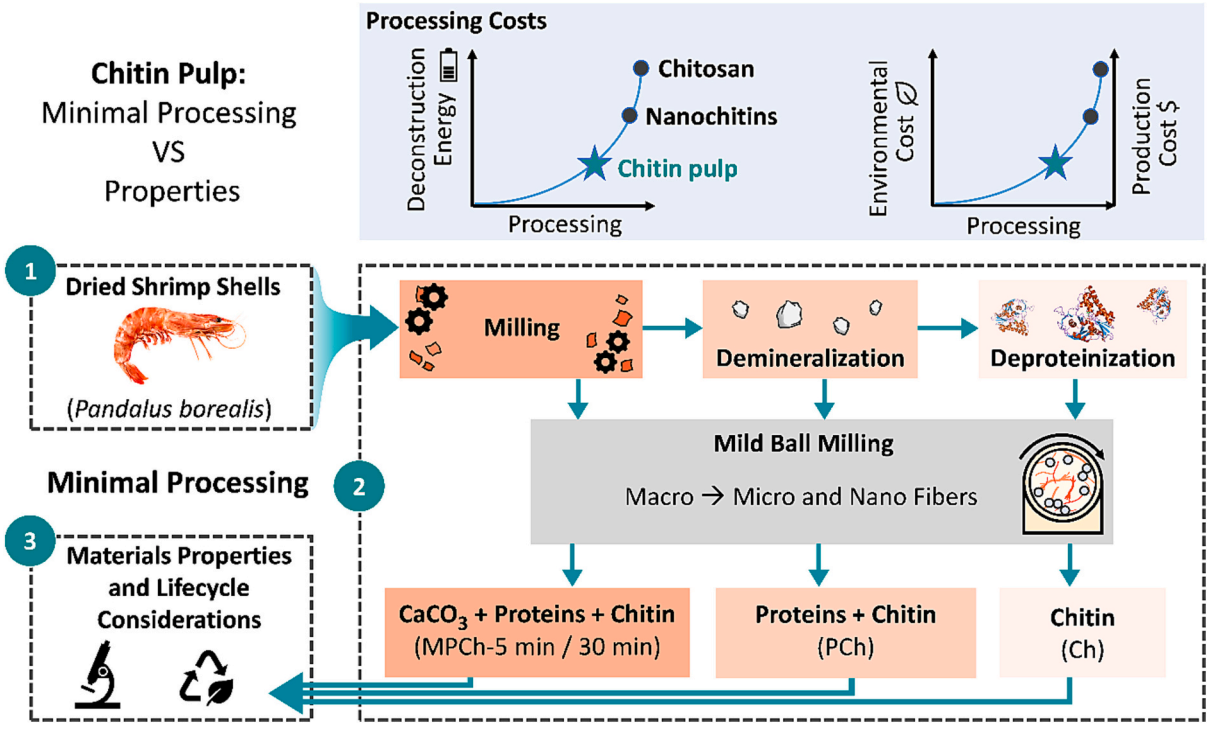

Fig. 1. The top panel illustrates the energy, environmental, and economic costs associated with the chitin pulp processing. The panels within the dashed lines represent the processing routes applied in this work, aimed at analyzing the minimal processing routes for chitin-based materials. In short, (1) dried shrimp shells are used to evaluate the effect of (2) demineralization, deproteinization, and defibrillation using ball milling on the final (3) material properties and sustainability of the process. Films made from samples acquired after every step described in (2) are analyzed herein.

human toxicity, land use and water use, or particulate matter formation, helping to understand the trade-offs in different categories, providing the holistic picture of the environmental sustainability of the chitin pulp (Lapuente Díaz de Otazu et al., 2021). As a summary, the implementation of LCA to minimal processing of chitin-pulp processing into films showcases the associated environmental impact metrics and benefits in comparison to traditional chitin processing routes (Yang et al., 2019).

2. Materials and methods

2.1. Shrimp shells pulp preparation

Frozen *Pandalus borealis* shrimps (Royal Greenland) shells were peeled, washed with deionized water, and dried overnight (~13 h) at 60 °C. Subsequently, the material was ground using a Culatti Micro Hammer Mill (DFH48) until a fine dust was collected (size ~60 mesh – 250 μm). Part of the milled shells were demineralized using 0.25 M HCl at a 1:40 ratio (solids: liquid) for 3 h while stirring. The resulting pulp was washed with deionized water using *ca.* 4 times the volume of the demineralization step. Part of the resulting pulp was deproteinized using 1 M NaOH, at the same 1:40 ratio, during 26 h while stirring. The pulps were then washed with deionized water using 4 times the liquid volume of the deproteinization step.

Part of the finely ground shrimp shells (non-demineralized and non-deproteinized) were ball milled (using a Fritsch Pulverisette 6) at pH 2 for 5 and 30 min. The solid to liquid ratio was maintained at 1:10 by suspending 3 g of the dried milled shells in 23 mL water, while *ca.* 7 mL 1 M HCl was used to adjust the pH. The ball milling was carried using 400 rpm and 24.9 g of 1 mm diameter and 46.66 g of 5 mm diameter zirconium oxide spheres. The purified and partially purified wet pulps were subjected to the same ball milling procedure for 30 min. In sum, the different samples generated using ball milling are classified under the following conditions and nomenclature (Fig. 1 and Table 1):

1: Non-demineralized and non-deproteinized pulp after 5-min ball milling (chitin pulp containing minerals, proteins and chitin, termed as **MPCh-5 min**).

2: Non-demineralized and non-deproteinized pulp submitted to 30-min ball milling (chitin pulp containing minerals, proteins and chitin, termed as **MPCh-30 min**).

3: Demineralized and non-deproteinized pulp submitted to 30-min ball milling (chitin pulp containing proteins and chitin, termed as **PCh**).

4: Demineralized and deproteinized pulp submitted to 30-min ball milling (chitin pulp containing only chitin, termed as **Ch**).

2.2. Film preparation.

The obtained pulps were used for preparing free-standing films through a dewatering process using a filtration unit equipped with a pressurized vessel operating at 1.5 bar. We used pulp suspensions at 0.4 wt% and pH 2, and two types of filters were used, *i.e.*, a Durapore® polyvinylidene fluoride (PVDF) hydrophilic membrane filter (124 mm diameter and 0.22 μm pore size) and a Sefar Nitex® fabric (code: 03–1/1, having a 1 μm pore size). The filter having smaller pore size was necessary when the filtrate was not perfectly transparent while using the Sefar filters. After the filtration step was complete, the wet cakes were removed from the filtration unit and placed on top of blotting paper and a stainless-steel sheet (1 mm thickness), as typically used for paper handsheet making. A layer of the Sefar filter was then placed on top of the wet cake and the blotting paper and metal sheet were put on top of the Sefar. Both metal plates were in contact with the hot press that was operated at 100 °C and 2000 psi (maintained by an Enterpac RC-Series Duo, P392, and hydraulic hand pump) for 50 min. The time needed for filtration corresponded to 25 min, 25 min, 10 h (overnight) and 10 min for chitin pulps produced by Conditions 1, 2, 3 and 4, respectively.

Table 1
Material and energy input inventory.

	Material	MPCh-5 min	MPCh-30 min	PCh	Ch
Inputs	Dried shrimp shells, g	3.000	3.000	6.000	15.000
	HCl (37 %), g	0.851	0.851	21.800	21.800
	NaOH (pellets, 99.9 %), g	–	–	–	12.000
	Deionized water, L	0.930	0.930	1.780	2.810
	Electricity, kWh	2.723	3.140	3.380	5.460
Outputs	HCl, g	0.851	0.851	26.370	26.370
	NaOH, g	–	–	–	24.000
	Waste water, L	0.930	0.930	1.780	2.810
	Proteins as dissolution by-product, g	–	–	–	5.700
	Lipids as dissolution by-product, g	–	–	0.06	0.06
	Dissolved $CaCO_3$, g	–	–	2.280	5.700
	CO_2 from $CaCO_3$	–	–	2.531	6.327
	H_2O from $CaCO_3$	–	–	0.410	1.026
	CO_2 from $CaCO_3$	–	–	1.000	2.510
	Film, g	3.000	3.000	3.000	3.000

2.2. Morphology, chemical and structural properties

Electron microscopy images were taken from the samples using a Zeiss SigmaVP, Germany, field emission scanning electron microscope (SEM) coupled with an energy-dispersive X-ray spectrometer (EDX). For surface images the SEM was operated at 2 kV, while for cross section images it was operated at 1.6 kV, both at working distances of *ca.* 4 mm and acquiring secondary electrons. For the EDX, it operated at 10 kV. Attenuated Total Reflectance-Fourier Transform Infrared (ATR-FTIR) spectra from the films were collected using a PerkinElmer Spectrum Two spectrometer. The measurements were done from 400 to 4000 cm^{-1}, with a resolution of 0.5 cm^{-1}, in duplicates of 16 scans. X-ray diffraction (XRD) was measured using a bench beamline SAXS/WAXS device (Xeuss® 3.0C, Xenocs SAS, Grenoble, France). The generator worked at 45 kV and 200 mA, with Cu Kα radiation. Oven dried squared film samples (L = 5 mm) were measured in transmission mode with a working distance of 55 mm, calibrated using LaB_6 diffraction pattern. The background correction was done by subtracting the scattering of an empty sample holder using SasView 5.0.3 software.

2.3. Water absorption and mechanical properties

Static water contact angle measurements were performed using a Theta Flex optical tensiometer (Biolin Scientific), where the reported values are based on the average and standard deviation of triplicates acquired at different positions of the same film. Each individual measurement was performed using deionized water and based on images recorded during the 60 s following the first contact between the droplet and the film surface. The image frame rate was set at one frame per second.

The mechanical properties of the dry and wet films were measured using an MTS 400 (MTS Systems Norden) universal mechanical testing unit operating at 0.3 $mm{\cdot}min^{-1}$ and using a gauge length of 20 mm. All specimens were cut using a sharp razor blade to achieve their final dimensions, *i.e.*, 5 mm wide and 40 mm long. All tests were conducted at 50 ± 3 % relative humidity and 22 ± 1 °C. All samples were acclimatized at such temperature and humidity for at least 48 h prior to testing. To assess the mechanical properties of wet films and their water retention capacity, the samples were submerged for 24 h in deionized water and only removed immediately before the test. Before mounting the specimens in the tensile tester, excess water was removed by lightly touching the specimens in paper towels. The mass of the samples before this soaking period was compared with that of dry films equilibrated at the dry testing conditions.

2.4. Life cycle assessment (LCA)

LCA was carried out following the International Standards ISO 14040

and ISO 14044.[29] Accordingly, we quantified the *cradle-to-gate* environmental impacts of chitin-pulp extraction and it's processing into films. Three different methods with an increasing extent of processing were considered:

1. ball milling + hot pressing to render **MPCh** pulp (comprising minerals, proteins, lipids and chitin).
2. ball milling + demineralization + hot pressing to render **PCh** pulp (comprising proteins and chitin).
3. ball milling + demineralization + deproteinization + hot pressing to render **Ch** pulp (comprising chitin).

As the second phase during a LCA, the life cycle inventory (LCI) considering the input data is briefly defined and shown in Table 1 to enable future comparison and follow-up work (additional details are provided in Tables S1-S4) (Laurent et al., 2020). The relatively small energy consumption differences obtained originate from the very low power consumption of the Fritsch Pulverisette 6 milling (1000 W). Further details on the process are shown in the flowchart in Fig. S1. To conduct the analysis, material quantities, the electricity for *on-site* production and the emissions were contemplated (the database also considered upstream production). The electricity mix of the European Network of Transmission System Operators (ENTSO-E) accounting for the electricity across Europe was used to extrapolate obtained results in Europe.

The quantity of dissolved material ($CaCO_3$, proteins and lipids) was estimated based on the amount of obtained films together with the theoretical composition of dried *Pandalus borealis* shells (~38 wt% protein, ~38 wt% $CaCO_3$, ~20 wt% chitin, ~0.4 wt% total lipids) (Rødde, Einbu, & Vårum, 2008). Other by-products were not considered due to their low weight fraction (*i.e.* astaxanthin: 14–39 mg/kg). Regarding completely dissolved by-products, we also considered that the HCl-induced chitin demineralization happens *via* $CaCO_3$ decomposition into $CaCl_2$ and CO_2 as (Santos et al., 2020):

$$2HCl + CaCO_3 \rightarrow CaCl_2 + H_2O + CO_2\uparrow.$$

or

$$0.73\ g\ HCl + 1\ g\ CaCO_3 \rightarrow 1.11\ g\ CaCl_2 + 0.18\ g\ H_2O + 0.44\ g\ CO_2\uparrow$$

In the third phase, the life cycle impact assessment (LCIA) was carried out to quantify the impacts. To do so, OpenLCA software with the ecoinvent v3.8 database (released on September 2021) was used. The ReCiPe 2016 Midpoint (H) method considered 18 environmental impact indicators. This method is widely accepted,(Prado et al., 2020) and provides additional metrics (such as water consumption) in comparison to other approaches. Usually, physical parameters that reflect the main characteristics of the product being analyzed are set as the functional unit (FU) during LCA. Following the recommendations regarding LCA multi-functionality problems (Pelletier, Ardente, Brandão, De Camillis, & Pennington, 2015), a FU based on mass was considered given its "relevant underlying physical relationship". Accordingly, 1 g of processed film was set as the FU. The fourth phase of the LCA procedure, the interpretation, is discussed in the next section.

3. Results and discussion

To evaluate the effect of mild processing conditions during the production of chitin pulp films and the compositional synergies within the resulting materials, raw shrimp (*Pandalus borealis*) shells were dried, ground, and subsequently used to obtain films having thicknesses of *ca.* 100 μm as summarized in Fig. 1. The resulting pulps were used to make films *via* vacuum filtration and hot pressing. The obtained films were characterized for their morphology, water absorption and wetting, mechanical properties, and associated environmental impacts *via* life cycle assessment.

3.1. Chitin pulp morphology

We firstly explored the effect of ball milling on film formation and elemental composition. Fig. 2a,b reveals substantially different levels of homogeneity after 5-and 30-min ball milling. The darker color on the top of the films (air side) is indicative of a higher local protein concentration compared to that on the brighter bottom (filter side) of the films. Energy dispersive X-ray analysis (EDX, Fig. 2a3 and Fig. 2b3) over areas of at least *ca.* 2 mm^2 confirm a larger amount of protein at the air side (top surface). Considering that fully acetylated chitin has a nitrogen content of 6.89 wt%, and the nitrogen content in proteins is roughly 16 wt% (slightly depending on the amino acid composition) (Díaz-Rojas et al., 2006), the larger nitrogen content at the air sides for both samples reflects an accumulation of proteins (Boulos, Tännler, & Nyström, 2020) According to previous analyses in the field, the nitrogen concentration of 11.2–12.9 wt% at the film surface corresponds to approximately 58.0 wt % proteins (Díaz-Rojas et al., 2006). The average nitrogen content decreases from 11.2 wt% to 9.2 wt% upon extending the ball milling period from 5 to 30 min. This is possibly a result of the improved homogeneity of distribution of the $CaCO_3$ particles within the film and at the bottom side of the film generated after 30 min ball milling (Fig. 2b).

The asymmetric distribution of proteins (two-sidedness of the film) was also evidenced by EDX analysis of the films originating from the demineralized pulp (Fig. 2c,d), although no significant color difference was noted when comparing both sides. Importantly, the **PCh** sample (Fig. 2c) presents the darkest color and the highest nitrogen content among all samples, indicating larger protein content and the removal of the inorganic matter. The demineralized and deproteinized film (**Ch**) presents the highest level of homogeneity between sides, with a low nitrogen content (5.0–5.7 wt%), matching that of chitin (Fig. 2d). This is an indication that the treatment used herein was enough to generate chitin pulp of relatively high purity. Attenuated total reflectance-Fourier transform infrared (ATR-FTIR) spectra in Fig. S2, and X-ray diffraction (XRD) patterns (see Fig. S3 and corresponding discussion) confirm the presence of α-chitin and the removal of $CaCO_3$ and proteins from the films (Sampath et al., 2022).

Cross section and plane view SEM images were obtained to reveal details on the morphological characteristics of the chitin pulp films. The top row in Fig. 3a,b,c shows the occurrence of a smooth protein layer covering the air side surface of the chitin pulp films in combination with small patches of uncovered fibers. In contrast, the air side of the deproteinized sample in Fig. 3d is mainly composed of chitin nanofibrils, although certain protein-covered areas are visible. As shown in the filter side of the sample ball milled for 5 min (Fig. 3a, lower inset), a short ball milling time cannot completely break the large $CaCO_3$ particles. As a result, the inorganic particles of *ca.* 10 μm quickly sediment during filtration, which explains the higher inorganic content at the filter side of the film (Ca concentration of 1.7 and 4.7 wt% for air and filter sides, respectively). When the ball milling is extended to 30 min (Fig. 3b), $CaCO_3$ particles and their aggregates are broken into smaller pieces, increasing their dispersion stability to yield films with enhanced homogeneity across the film thickness after filtration (Ca concentration of 8.5 and 9.4 wt% for air and filter sides, respectively). Still, a few large aggregates of *ca.* 3 to 5 μm are present, although in lower quantities than in the sample treated for shorter times.

The size of the chitin fibers and aggregates forming the films is also reduced upon increasing the ball milling time, as can be seen in the cross-section images of the films (Fig. 3a,b bottom row). In addition, smaller fibers and aggregates facilitate the assembly into a compact structure upon filtration, decreasing the amount of voids within the film. To compare the differences between samples of different compositions, the 30 min treatment was selected. Interestingly, the cross-section SEM images in Fig. 3b,c,d show that the protein containing samples also form a more compact structure and a flatter fracture surface, in a macroscopic scale, if compared to the film solely composed of chitin. These results suggest that the proteins fill the interfibrillar space, conferring a

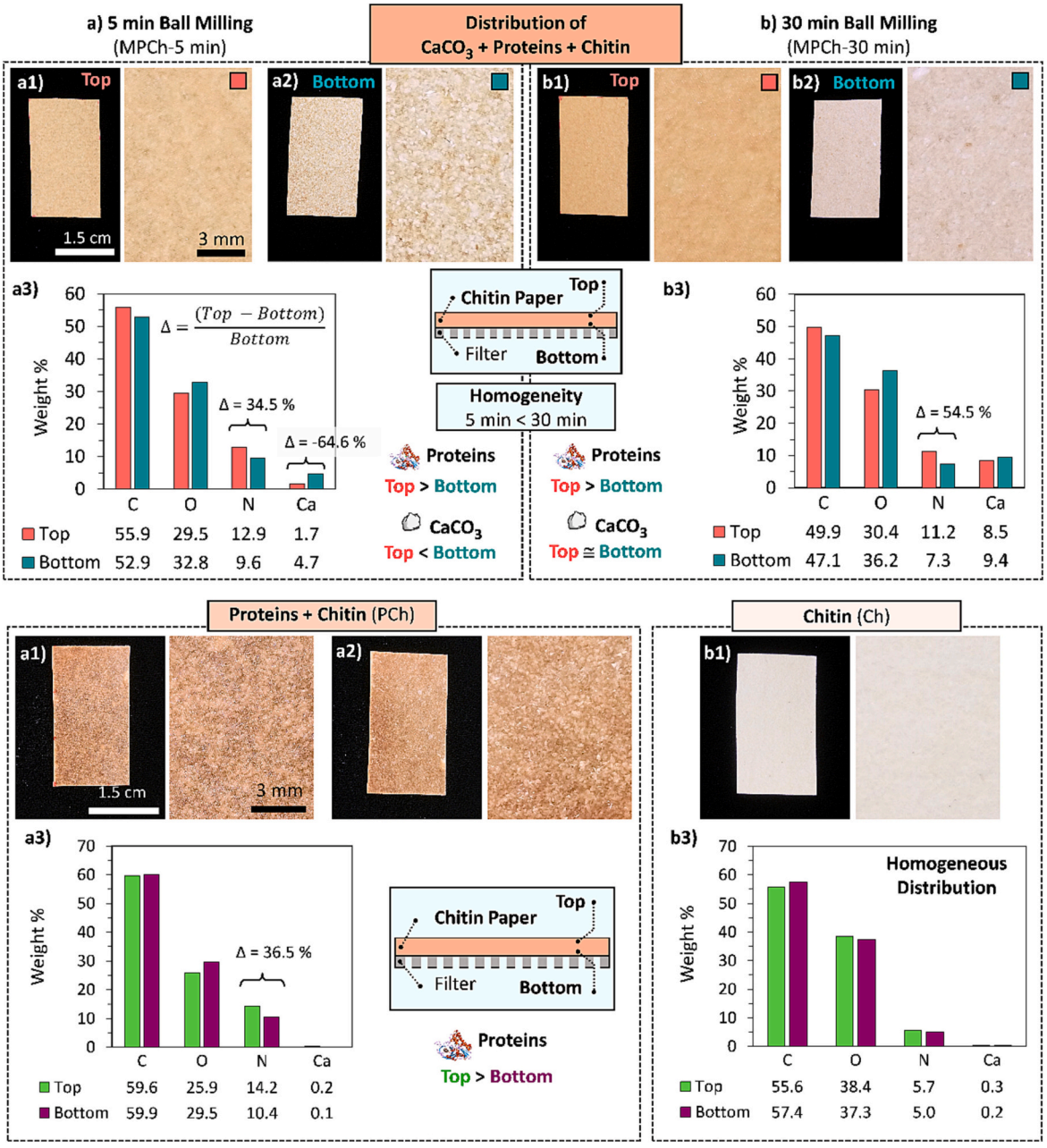

Fig. 2. Digital photographs depicting the sidedness of chitin-pulp films as assessed by the different distribution of $CaCO_3$, proteins and chitin a) 5-min and b) 30-min ball milling. The elemental composition by weight for the air and filter sides of the film is shown in a3 and b3; c) demineralized film produced from 30-min ball milling and d) demineralized and deproteinized film generated from 30-min ball milling.

composite character to the films and thus increasing the binding between chitin fibrils similar to what naturally occurs in crustacean exoskeletons (Lizundia et al., 2021). A similar behavior has been recently reported in chitin nanopapers extracted from mushroom (Fazli Wan Nawawi, Lee, Kontturi, Murphy, & Bismarck, 2019).

In summary, differences in composition between opposite sides of the films may originate from the filtration process that leads to an inhomogeneous material distribution depending on the components. A similar behavior is observed during papermaking, where fines, fillers and fibers form a layered structure with different composition in the out-of-plane direction (Fischer et al., 2017; Taipale, Österberg, Nykänen, Ruokolainen, & Laine, 2010). The contribution of the surface activity of the proteins and their colloidal stability are also factors that likely influence their accumulation on the surface. Importantly, such two-sidedness of the films, *i.e.* in terms of composition and morphology, may be further explored for applications. For instance, such an effect can be used in the development of films that are asymmetric or with compositional gradients, which are normally difficult to produce by chemical reaction (Razza, Castellino, & Sangermano, 2017) or specialized equipment/process (Cheng et al., 2016). In this way, chitin pulp films could be explored in the near term as substitutes for bilayer polymeric films used in the packaging industry (general purpose) given their film-forming ability (Jin, Liu, Lam, & Moores, 2021; Scaffaro, Maio, Gulino, Di Salvo, & Arcarisi, 2020).

3.2. *Water contact angle and water absorption*

As summarized in Fig. 4a, the static water contact angle at the top surface of the chitin pulp films can be modified by almost 55° depending on the composition. In particular, the pure chitin pulp film (**Ch**) is the

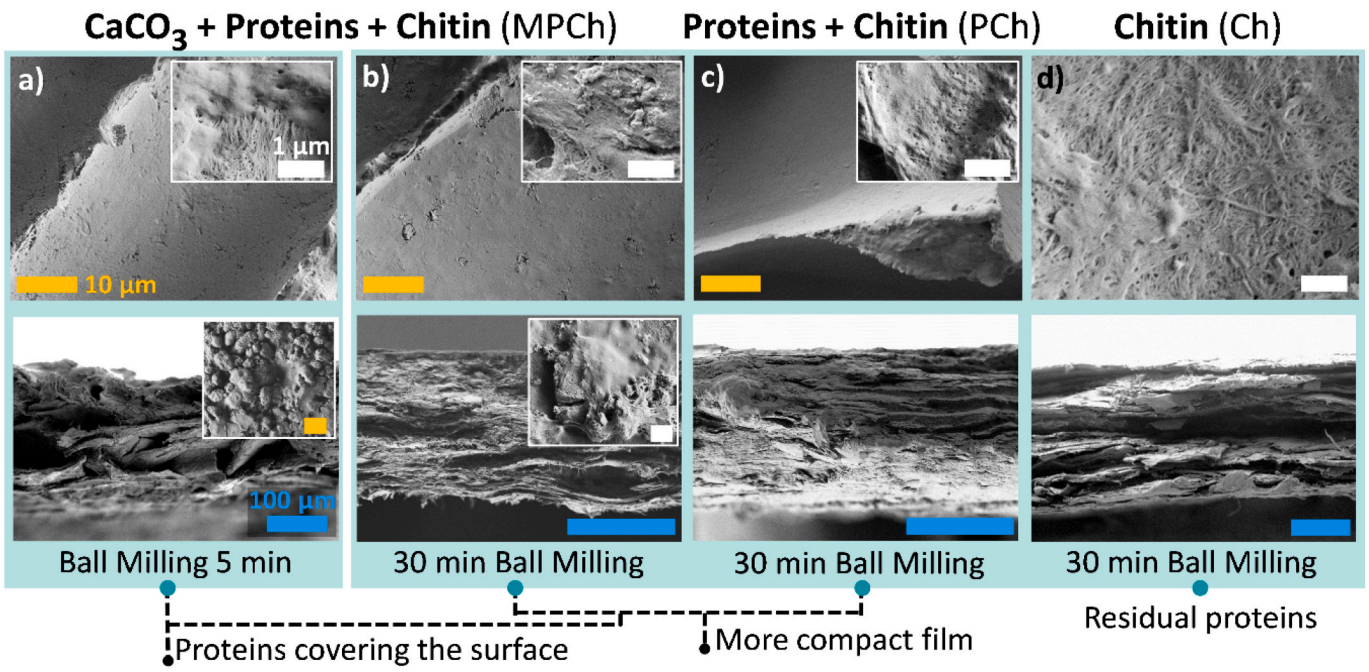

Fig. 3. Images (cross section and plane view) to assess the morphology of films obtained from chitin pulp. Top row: SEM images of the air side of films generated with chitin-based pulps having different compositions and ball milling treatment times. The insets of the images in the top row depict the layer immediately below the air side of the films. They include a) fibers and proteins coexisting in the 5-min ball milled sample; b) $CaCO_3$, proteins and fibers in the sample ball-milled for 30 min; c) proteins and fibers in the sample subjected to demineralization and 30-min ball milling. The bottom row depicts the cross sections of the films, and the lower insets show the $CaCO_3$ particles and aggregates at the filter side of the films ball milled for a) 5-min and b) 30-min. The white scale bars are 1 µm, those in yellow are 10 µm, and those in blue are 100 µm.

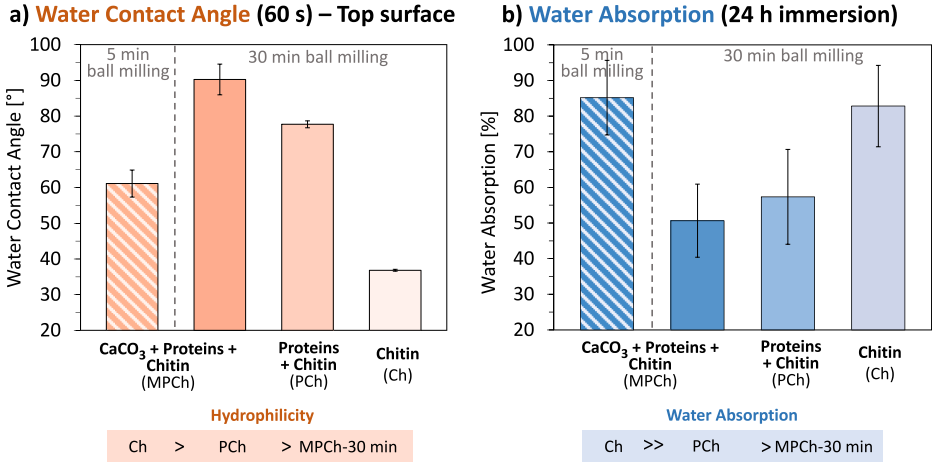

Fig. 4. a) Water contact angle after 60 s and b) water absorption after 24 h immersion in water for chitin-pulp films.

most hydrophilic as indicated by the low contact angle of 37 ± 1°. Interestingly, the film generated from the pulp processed during 30 min ball milling (**MPCh-30 min**) presents the highest water contact angle with a value of 90 ± 4°, which is slightly superior to common types of plastics (poly(L-lactide), poly(ethylene terephthalate)) found in food packaging (Dil et al., 2018; Lizundia, Ruiz-Rubio, Vilas, & León, 2016). Although this film contains chitin and $CaCO_3$, which are inherently hydrophilic, the protein layer formed at the surface make the film hydrophobic. This hydrophobicity could be ascribed to the presence of terminal hydrophobic amino acids at the film surface, which in turn prevents extensive water infiltration and subsequent absorption during the 24 h immersion test (Fig. 4b). Specifically, a water absorption value as low as 50.6 ± 10.3 % is obtained. The sample with the highest protein content (**PCh**) generates the second most hydrophobic film, with water contact angle and absorption values of 78 ± 1° and 57 ± 13 %, respectively. This is possibly caused by damages to the topmost protein layer when removing the film from the filters after hot pressing. Also, the smaller dimensions of the chitin fibers in the film could have contributed to their increased presence at the surface of the film, thus slightly increasing water absorption and decreasing the water contact angle values.

Importantly, as shown in earlier sections, large $CaCO_3$ particles present in the 5-min ball milled sample (**MPCh-5 min**) reduce the homogeneity of the protein layer at the film surface, which in turn increase the water affinity of the films. Particularly, the average water contact angle and the water absorption are 61 ± 4° and 85 ± 10 %, respectively. Despite the higher water contact angle, the water absorption was nearly the same as that for chitin alone. This is possibly caused by the large

inorganic particles and aggregates exposed at the filter side of the film, which were not present in the other protein-containing samples. These results show the tunability of water interactions in chitin pulp films, within a wide window, through relatively simple processing, avoiding the need for multi-step and environmentally harmful chemical modification approaches to tailor hydrophobicity (Gopalan Nair, Dufresne, Gandini, & Belgacem, 2003; Kiliona, Zhou, Zhu, Lan, & Lin, 2020).

3.3. Mechanical strength

The different morphological and water-interaction characteristics discussed in earlier sections are also expected to affect the dry and wet mechanical properties of the samples. Uniaxial tensile tests were conducted on chitin pulp films and the obtained results are summarized in Fig. 5 and Fig. S4. As observed in Fig. 5a, the largest ultimate strength, at 93.3 ± 7.3 MPa, was observed for the **PCh** films produced upon demineralization and 30-min ball milling. The second strongest film, at 45.1 ± 10.8 MPa, is that from pulps containing minerals, proteins, and chitin after 30-min ball milling (**MPCh-30 min**). The purified chitin film (**Ch**) and the sample ball milled for 5 min (**MPCh-5 min**) generated substantially weaker materials (25.1 ± 6.8 MPa and 17.5 ± 4.3 MPa, respectively). The wet strength was assessed, and the same trend was observed although the relative differences between pulps were more pronounced. Particularly, the **PCh** film composed of chitin and protein failed at 7.7 ± 0.4 MPa, which represents a four-fold increase over the second strongest sample, *i.e.*, the film composed of minerals, proteins and chitin ball-milled for 30 min.

As seen in Fig. 5c, the strain at break for the demineralized sample (**PCh**) was at least twice as high if compared to nearly all other films, with the dry and wet conditions displaying 1.3 ± 0.1 % and 1.4 ± 0.2 %, respectively. Together with the higher tensile strength, this resulted in films that are, respectively, up to four and eighty five times tougher than the mineral containing film or to the completely purified chitin film in wet conditions. Furthermore, the film made out of the 30-min ball milled pulp and containing the mineral phase (**MPCh-30 min**) displayed the highest elastic modulus, with 9.4 ± 1.7 GPa. The **PCh** film containing only proteins and chitin was the second highest, with 7.9 ± 0.6 GPa, while the other two conditions (*i.e.* the 5-min ball milled pulps, and purified chitin) displayed values closer to 5 GPa. Overall, these results can be explained based on the compositional and morphological characteristics discussed in earlier sections, where the processing-structure-property relationship can be summarized as follows:

- longer ball milling times reduce $CaCO_3$ particle size (increase $CaCO_3$ available surface area and interactions with the matrix) and improve film homogeneity, which in turn enhances the stress transfer

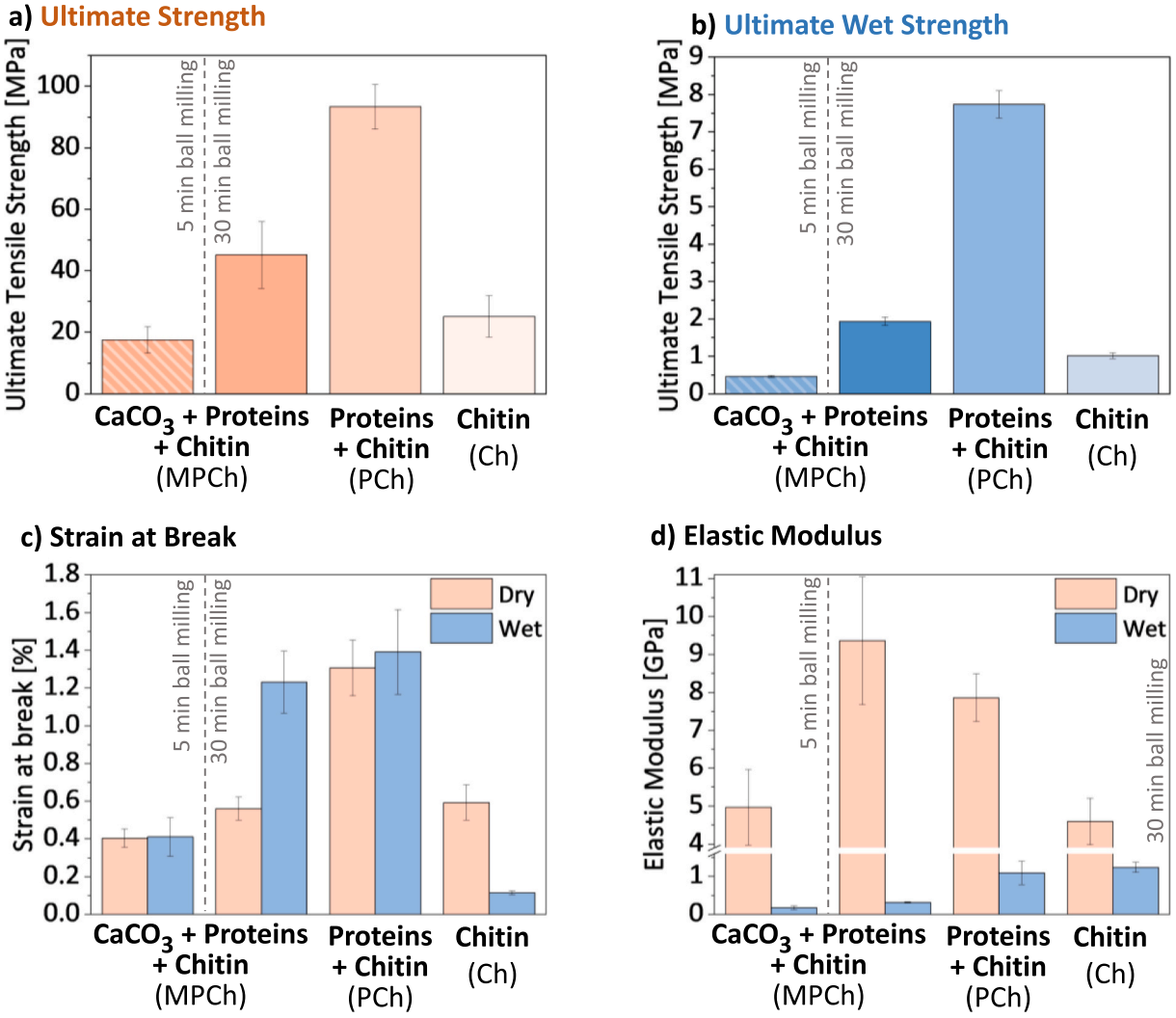

Fig. 5. Tensile mechanical properties of the films generated from chitin pulps having different compositions and subjected to different ball milling times. a) Ultimate strength; b) ultimate wet strength; c) strain at break and d) elastic modulus. Representative stress strain curves and the work of fracture for each film composition are showcased in Fig. S4.

between the particles and the matrix, as found in particulate-polymer composites (Fu, Feng, Lauke, & Mai, 2008).

- further removal of the inorganic phase favors protein-chitin interactions, with an enhanced binding action between composite constituents through histidyl and aspartyl residues (Raabe et al., 2006). In this case, proteins provide an efficient interfacial adhesion between nanofibrils just as they do in the extracellular matrix of crustaceans (Chen, Lin, McKittrick, & Meyers, 2008) A similar trend has been recently observed by Nawawi et al., where chitin nanopapers having amorphous glucans (polysaccharides derived from D-glucose) displayed improved binding between the nanofibrils (Fazli Wan Nawawi et al., 2019). Interestingly, new structures and properties are envisioned if the proteins or mineral particles are used as templates and (partly) removed after filtration, either before or after pressing. In such case, micro- and nanopores would be generated, providing an interesting platform for the production of, *e.g.*, membranes.
- further purification prior to ball milling yields chitin fibrils lacking efficient binding, as evidenced by the voids between layers within the film (see SEM micrograph in Fig. 3d). This is likely a result of the larger fibers and fiber aggregates prior to film formation, as well as of the absence of proteins. The randomly distributed small-sized pores originating from the HCl wash potentially damage the mechanical properties under tensile loading, acting as sites for crack initiation and increasing material brittleness (Huang, Yang, Chen, Li, & Zhai, 2019).

In summary, from an application standpoint where high mechanical properties and water resistance are important, *e.g.* in single use plastics or fiber-reinforced composites, the most appropriate balance of minimum processing *vs* properties can be achieved by keeping the proteins naturally present in the sourced material. However, allergenicity concerns should be addressed before the actual implementation of chitin-pulp materials in *e.g.* the food packaging industry. In particular, routes to remove or degrade the protein responsible for shellfish allergies, tropomyosin, should be considered. Among those, ultrasound or high temperature-pressure treatments, respectively, are promising strategies for degrading tropomyosin or generating Maillard reaction, when in the presence of reducing sugars, thus reducing allergenicity (Lu, Cheng, Jiang, Lin, & Lu., 2023). Accordingly, the hot-pressing process used in the present study may have been beneficial in an eventual food packaging context. Therefore, optimal treatment temperatures, pressures, and additives for reducing allergenicity and improving film properties, *e.g.* hydrophobicity, should be explored in future studies.

Importantly, despite of the wide range of extensive mechanical treatments often employed for cellulose- or chitin-based pulps, *e.g.*, disintegration and mechanical beating (Sehaqui, Berglund, & Zhou, 2013), ball milling was used herein to keep the processing steps to a minimum while attaining the tensile strength values comparable to those observed in literature for chitin-based nanopapers. Mushi et al. (Mushi, Butchosa, Zhou, & Berglund, 2014), for instance, achieved values of 77 MPa when using protein-containing (7 % residual proteins) chitin nanofibrils having diameters in the range of 70–150 nm after 5 passes of microfluidization. More recently, Wu et al. used an overnight refining operation followed by microfluidization to mechanically process squid pens into highly homogeneous chitin nanofibril suspensions used for making nanopapers, reaching strength values of more than 250 MPa (Wu, Jungstedt, Šoltésová, Mushi, & Berglund, 2019). Despite of the extensive processing required for such refined materials, only few applications require such levels of high strength. Most synthetic rigid plastics, for instance, hardly reach *ca.* 100 MPa of ultimate tensile strength and more than 7 % elongation at break (Sarkanen, Chen, & Wang, 2016). In addition, biodegradable polyesters, either synthetic or bio-based, very rarely exceed ultimate strengths of 60 MPa (Manavitehrani et al., 2016), not to mention that water-soluble cellulose derivative films present ultimate tensile strength values below 55 MPa (Rincon-Iglesias, Lizundia, & Lanceros-Mendez, 2019). or the fact that the majority of commercially available cellulose-based papers presenting lower mechanical performance (Li et al., 2021; Tardy et al., 2021). The relatively low strains at break achieved in the present work, however, is a limitation. Nevertheless, the pulp and paper industry has mastered a range of simple mechanical pulping and refining techniques (Mboowa, 2021), that lead to breaking strains of more than 15 % (Khakalo, Kouko, Filpponen, Retulainen, & Rojas, 2017). Moreover, the effect of proteins in this context can be further studied given their role in bonding and possible plasticization effects (Khakalo, Filpponen, & Rojas, 2017; Khakalo, Vishtal, Retulainen, Filpponen, & Rojas, 2017; Strand et al., 2017). Finally, the levels of purity and defibrillation most often aimed when processing chitin-based materials into highly purified chitin nanofibers might not be justifiable when, for instance, replacing single use plastics or in the development of barrier properties.

3.4. Environmental impact assessment and cost estimation

To determine how the minimal treatment processes here developed are translated into materials with improved environmental sustainability, the *cradle-to-gate* environmental impacts per 1 g of film have been calculated according to LCA; as summarized in Table 2. Note that the production-scaling assumptions for this study and the comparative analyses are provided in the table caption. To shed more light on the potential of the developed approach and cross-compare the obtained impacts with related materials having potentially comparable uses, the environmental impacts corresponding to representative and analogous bio-based materials are also disclosed (few representative works are included due to methodological differences). The global warming potential (GPW, quantified in equivalent CO_2 emissions) category is firstly analyzed given its role as the main indicator. According to the LCA results, the **MPCh-5 min** film production (considering material use, mechanical/chemical treatment and electricity consumption) bears a CO_2 footprint of 341.6 g CO_2-equiv.$\cdot g^{-1}$. This process includes drying, grinding, ball milling, filtration and the final processing into films by hot pressing. The impacts are slightly enhanced up to 393.8 g CO_2-equiv.$\cdot g^{-1}$ extending the milling time to 30 min due to the larger energy demand. For the **PCh** film, where additional demineralization and filtration steps are applied, the GWP increases to 433.0 g CO_2-equiv.$\cdot g^{-1}$. Finally, the pure chitin film (**Ch**), which incorporates a deproteinization step with a centrifugation and filtration to yield the raw chitin-film, presents a notably larger CO_2 footprint of 706.0 g CO_2-equiv.$\cdot g^{-1}$. Such larger impact originates from its marked chemical (with additional 24 g of NaOH) and energy consumption.

The results for protein-rich chitin pulp are below the impacts disclosed in a recent study, where the sole process of chitin nanocrystal (ChNC) isolation from shrimp shells, excluding its processing into free-standing films, bears a footprint of 906.8 g CO_2-equiv.$\cdot g^{-1}$ (*cradle-to-gate*, ReCiPe 2016 Midpoint H method) (Berroci, Vallejo, & Lizundia, 2022). Fibrillation approaches could potentially reduce the impacts of bio-based colloid isolation given the fact that extensive use of chemicals is avoided. However, still large impact values of 810.7 g CO_2-equiv.$\cdot g^{-1}$ are reached (example of cellulose nanofibrils, CNFs) (Turk et al., 2020). Comparing these impacts with the results corresponding to another biopolymer extracted from shrimp shells, chitosan, could help to better understand the environmental feasibility of the chitin-pulp films. In this context, Riofrio et al. recently estimated a GWP of 59.2 g CO_2-equiv. per 1 g of chitosan extracted from *Ecuadorian shrimp* shell (Riofrio, Alcivar, & Baykara, 2021). Although the results are normalized here using the same functional unit of 1 g, and both Berroci et al. (for ChNCs) and Riofrio et al. (for chitosan) applied a similar *cradle-to-gate* approach based on the ReCiPe Midpoint H method, the production scale considered is notably different. As a matter of fact, 125 g of water-dispersed ChNCs were considered for process up-scaling by Berroci et al. (from an initial 1 kg of crustacean exoskeleton), while the chitosan production was up-scaled to be at 1 kg scale (from an initial 35 kg of shrimp shell),

Table 2
Environmental impacts in 18 impact indicators for 1 g of film according to ReCiPe 2016 (H). Chitin nanocrystals from shrimp (ChNC) and cellulose nanofibril (CNF).

Impact category	MPCh-5 min[a]	MPCh-30 min[a]	PCh[a]	Ch[a]	ChNC [b] (Berroci et al., 2022)	Chitosan [c] (Riofrio et al., 2021)	CNF [d] (Turk et al., 2020)	Unit
Fine particulate matter	0.49667	0.57333	0.63667	1.04000	1.52000	6.07×10^{-5}	0.00220	kg PM2.5-equiv.
Fossil resource scarcity	91.30333	105.26667	115.41667	187.71333	248.71000	0.01131	0.40200	kg oil-equiv.
Freshwater ecotoxicity	11.19333	12.90000	14.76667	23.87000	40.29000	0.00112	0.02530	kg 1,4-DCB
Freshwater eutrophication	0.36000	0.41333	0.450000	0.726667	0.82400	1.39×10^{-5}	0.00080	kg P-equiv.
Global Warming Potential	341.61	393.85	433.03	705.98	906.77	59.22	810.70	g CO_2-equiv.
Human carcinogenic toxicity	22.57000	26.016667	28.66667	46.58667	63.54000	0.00131	0.04940	kg 1,4-DCB
Human non-carci. Toxicity	435.89000	502.40000	558.89000	904.57000	1232.99000	0.02818	1.05170	kg 1,4-DCB
Ionizing radiation	182.42667	210.36000	227.00667	367.49667	392.20000	0.00247	0.18050	kBq Co-60-equiv.
Land use	8.64666	9.96666	10.88000	17.65333	31.60000	0.00569	–	m^2a crop-equiv.
Marine ecotoxicity	15.41000	17.76000	20.27333	32.77000	54.15200	0.00155	0.03120	kg 1,4-DCB
Marine eutrophication	0.02767	0.03162	0.03666	0.05666	0.087	3.14×10^{-6}	0.00005	kg N-equiv.
Mineral resource scarcity	0.38333	0.44000	0.53666	0.86333	2.00300	1.09×10^{-4}	0.00075	kg Cu-equiv.
Ozone formation, human health	0.57333	0.660000	0.73000	1.19333	2.64400	7.98×10^{-5}	0.00301	kg NO_x-equiv.
Ozone formation, terrest. Ecosyst.	0.57666667	0.66666667	0.73666667	1.20666667	3.232	8.13×10^{-5}	0.00389	kg NO_x-equiv.
Stratospheric ozone depletion	0.00017111	0.0001972	0.00021864	0.00036052	651.30×10^{-6}	4.03×10^{-8}	2.12×10^{-7}	kg CFC11 equiv.
Terrestrial acidification	1.21000	1.39333	1.54333	2.50666	3.60500	1.97×10^{-4}	0.00644	kg SO_2-equiv.
Terrestrial ecotoxicity	309.12	355.86	464.69	745.35	2194.07	0.10	55.96	kg 1,4-DCB
Water consumption	6.606	7.610	8.400	13.733	21.440	0.034	0.028	m^3

and Turk et al. considered a 1 kg production of cellulose nanofibers (2.19 kg of thermo-ground wood pulp). This is in contrast with the laboratory-scale studies here performed aimed at 3 g film production (from an initial 24 g of shrimp shell). Accordingly, there is a need for further exploring approaches to translate the results into practical use, not only considering the techno-economic viability but the environmental sustainability and impacts of biomass processing, which could be lowered by a factor of 6.5 when up-scaling from 10 g to 50 kg (Katakojwala & Mohan, 2020). Therefore, it is reasonable to state that the introduced chitin pulp processing offers an opportunity for practical and viable implementation towards sustainable materials.

The LCA studies use the following production-scaling assumptions: [a]: 3 g production in the form of a film from an initial 24 g of shrimp shell; [b]: 125 g production in the form of an aqueous dispersion from an initial 1 kg of crustacean exoskeleton; [c]: 1 kg production in the form of a solution from an initial 35 kg of shrimp shell; [d]: 1 kg production in the form of an aqueous dispersion from an initial 2.19 kg of thermo-ground wood pulp.

To understand the full environmental profile of chitin-pulp films, additional impact categories should be observed. In this sense, water use results especially critical during biomass treatment given the fact that generated wastewater jeopardizes aquatic environments. In the case of the scenario bearing larger impacts, the **Ch** film, 13.73 m^3 of water (*water consumption* category) are required as opposed to the 21.440 m^3 needed for chitin nanocrystal isolation from shrimp shells. When confronting the impacts of **PCh** film (the one showing the best mechanical properties) against ChNCs, notably lower impacts are seen in the categories of *particulate matter formation* (0.6367 *vs.* 1.5200 kg PM2.5-equiv.), *fossil resource scarcity* (115.417 *vs.* 248.710 kg oil-equiv.), *terrestrial acidification* (1.5433 *vs.* 3.6050 kg SO_2-equiv.) and *ozone formation* (both human health and terrestrial ecosystems). These results highlight the environmentally benign character of the protein-rich chitin pulp isolation route here developed. In addition, **PCh** film bears a ~ 3-fold reduction in water use in comparison with chitin nanocrystals production. A possible route to further reduce solvent/water use and waste generation could be the solvent-free High-Humidity Shaker Aging approach (Jin et al., 2022). Although comparable impacts over chitosan are observed for several categories, the larger values achieved for *terrestrial ecotoxicity* or *human toxicity* (both carcinogenic and non-carcinogenic) indicate the need for further improvement.

The electricity consumption accounts for the largest share on the GWP for all the processes, exceeding 97 % as associated with the lab-scale production described herein, which corroborate with other reports on cellulose nanocrystals (Katakojwala & Mohan, 2020). In particular, the **MPCh** films have the largest share of the electricity, with a negligible contribution of water or chemicals. Ball milling emerges as the largest contributor energy-wise, so future work should be focused on the optimization (time reduction) of this process to reduce energy consumption. In addition, shifting from fossil-based to a 100 % renewable electric power supply (combination of solar, hydro-power, wind, biogas) can further lower the impacts in categories such as *acidification*, GWP, or *tropospheric ozone formation* (Lapuente Díaz de Otazu et al., 2021; Rödger et al., 2021). From the other side, the demineralization and deproteinization steps increase the GWP contribution of the whole process due to the use of additional water and chemicals (see PCh and Ch samples). However, their share still remains below 3 %, making electricity the prime contributor. The contribution of chemicals could be reduced by replacing the HCl by organic-acids. However, the trade-offs regarding leachant quantities should be carefully considered towards truly environmentally (and economically) sustainable processes because their use is not directly translated into lower impacts (Iturrondobeitia et al., 2022).

The consideration of the economic viability for chitin pulp production results essential towards actual application. As such, Table 3 summarizes the estimated costs for nanocelluloses and cellulosic pulp, paper/cardboard, and recycled cellulose pulp, together with their chitin analogues. In fact, a combination of environmental and economic sustainability will be required for the effective implementation of the processes here proposed as both environmental legislation and financial benefits are required for a thriving bio-based industry (Abbati De Assis et al., 2018). Considering obtained results, the purity of the shrimp shells may not be a limiting factor, so the processes could admit different shrimp species. The costs related to capital (initial equipment purchase) and operation processes (ongoing expenses originating from pulp-isolation) are expected to be relatively low for an up-scaled process.

Table 3
Summary of estimated costs for nanocelluloses, cellulosic pulp, paper/cardboard, and recycled cellulose based paper, together with their chitin analogues. Cellulose-based materials are highlighted in green, while chitin is highlighted in blue. [a] = Europe; [b] = Cost, insurance, freight, CIF to United States. [c] = Cost, insurance, freight, CIF to China.

Material	Estimated cost
Cellulose nanocrystals	~25.00 €·kg^{-1} (Inkwood Research, 2023)
Nanoscale fibrillated cellulose	~20.00 €·kg^{-1} (Li et al., 2021)
Southern bleached softwood kraft	0.06–0.10 €·kg^{-1} (Fastmarkets, 2023)
Northern bleached softwood kraft	0.06–0.10 €·kg^{-1} (Fastmarkets, 2023)
Papermaking-grade fibrillated cellulose	~0.60 €·kg^{-1} (Li et al., 2021)
Paper and cardboard [a]	0.18 €·kg^{-1} (Eurostat, 2023)
Paper other than graphic, packaging or tissue [b]	7.60 €·kg^{-1} (Indexbox, 2022)
Graphic papers [b]	1.10 €·kg^{-1} (Indexbox, 2022)
Old corrugated containers	0.05 €·kg^{-1} (Resource recycling, 2023)
Recycled brown pulp [c]	0.34–0.36 €·kg^{-1} (Fastmarkets, 2023)
Chitin nanocrystals	~ 11.90 €·kg^{-1} (Larbi et al., 2018)
Chitin nanofibrils	~ 6.70 €·kg^{-1} (Larbi et al., 2018)
Chitin pulp	~ 1.00 €·kg^{-1} (our estimations)

Our process for protein-rich chitin-pulp isolation uses conventional instruments readily available, such as a grinder or vacuum-assisted filtration equipment, which could be up-scaled to a mill coupled with an industrial filtration. Relatively cheap and abundant chemicals are used, with costs of 0.8 €·m^{-3} for water (Larbi et al., 2018), ~0.3 €·kg^{-1} for NaOH (Oladipo, Yusuf, Al-Ali, & Palmisano, 2021), or ~ 0.2–0.3 €·L^{-1} for 33 % HCl. In addition, these can be re-circulated to lower environmental impacts and increase profitability (Berroci et al., 2022). Besides, the amount of water used for raw chitin-pulp films results 2.5-times lower than that required for chitosan, which shows a production-cost of $8.4 to $12.0 per 1 kg under industrial scale processing (hundreds of ton of shrimp exoskeleton) (Gómez-Ríos, Barrera-Zapata, & Ríos-Estepa, 2017; Riofrio et al., 2021; Roberts, 2008). A recent work has also estimated the economics of the production for ChNCs isolated upon the environmentally-harsh acid hydrolysis of commercial shrimp shell α-chitin to obtain 11.9 € per kg of initial chitin, while this value drops to 6.7 € per kg of initial chitin for chitin nanofibrils (Larbi et al., 2018). Considering the use of 8.6 kg HCl and 2.1 m^3 water for washing (per kilo of initial chitin for ChNC isolation), this work suggests the potential marketability of value-added chitin-pulp. Moreover, as shown in Table 3, if up-scaled at industrial scale, as currently occurs for nanoscale fibrillated cellulose, a cost nearly or potentially below 1 € per kg of chitin pulp (dry basis) can be roughly estimated if tracing a parallelism to cellulose-based fibers, where a cost reduction of more than 20 times is observed when comparing cellulose pulp (0.60 € per dry kg papermaking-grade fibrillated cellulose) *vs.* nanocellulose (20.00 € per dry kg nanoscale fibrillated cellulose) (Li et al., 2021). Interestingly, chitin pulp could be recovered at the end of its useful life to be potentially sold as a secondary material in a similar way to the old corrugated containers, or to fabricated recycling chitin pulp (similarly to recycled cellulose brown pulp, 0.34–0.36 € per kg). Undoubtedly, these strategies closing material cycles would represent additional income and could improve the economics of a prospective chitin biorefinery.

4. Conclusions

Processing and application of chitin-based materials in large scale has been traditionally limited due to high financial and environmental costs, as *e.g.* associated with its processing into highly purified chitosan. By analyzing structure-property relationships and environmental impacts in light of LCA, this work demonstrates that minimally processed protein-rich chitin pulps can be a sustainable alternative for valorizing waste chitin.

First, chitin pulps were produced *via* mild ball milling of *Pandalus Borealis* shrimp shells treated to different levels of purity (*i.e.* untreated, demineralized, and demineralized and deproteinized). The pulps were then used to produce films, *i.e.* by vacuum filtration and hot pressing, which were subsequently analyzed to demonstrate the effect of each processing step on the properties of the materials formed. Film homogeneity was improved at longer milling times (5 min *vs* 30 min). Morphological observations of the top side of protein-containing films showed chitin nanofibrils covered by a smooth protein layer. In spite of the hydrophilic character of the isolated chitin films (water contact angle = 37 ± 1°; water absorption of 85 ± 10 %), non-chemically treated films having such protein layer were hydrophobic (contact angle of 90 ± 4° and water absorption of 51 ± 10 %). Cross-section images showed that the protein-containing films also presented a more compact structure, possibly caused by the proteins providing better bonding to layers of fibers, as well as by a higher defibrillation efficiency during ball-milling. Dry and wet ultimate strength values ranged from *ca.* 18 to 100 MPa and from *ca.* 0.5 to 8.0 MPa, respectively. These values are comparable to other biobased films, including some generated from nanofibers obtained upon extensive chemical and mechanical processing. With global warming potential values of 341.6–433.0 g·CO_2 equiv. per gram, protein-rich chitin pulp processing is environmentally preferred over more purified and processed versions of chitin (nano) materials, and presents merits to compete with chitosan after up-scaling.

Importantly, the chitin pulp here extracted requires low capital and operational costs as reflected by the use of conventional industrially available technologies and relatively lower needs of water, NaOH, HCl and electricity. With this in mind, chitin pulp films imply production-costs down below typical chitin nanocrystal or chitosan production processes, *i.e.* potentially reaching values as low as 1 € per kg. The mechanical performance of films in combination with low environmental impacts demonstrate the prospects of using minimally processed chitin pulp from crustacean shells to compete with commodity petroleum-based plastics or nanochitin papers obtained through extensive mechanical and chemical procedures. Besides, the process here developed can be extrapolated to other chitin sources, including fungi, insects, crustaceans and mollusks. In particular, when chitin is part of an exoskeleton, sources where the wall of the shell is thin are particularly interesting because it facilitates shorter milling, demineralization and deproteinization times. Optimally, when minerals are undesirable, fungi may be ideal sources as they require less processing to defibrillate and do not require demineralization. Importantly, all such sources generate a wide variety of proteins that may be explored in future studies to bring additional functionalities to the films. Finally, the water interaction and mechanical performance opens new opportunities for the application of chitin pulp for water treatment, general purpose packaging, or energy storage purposes.

CRediT authorship contribution statement

Luiz G. Greca: Conceptualization, Methodology, Formal analysis, Investigation, Supervision, Writing – original draft, Writing – review & editing. **Ainara Azpiazu**: Methodology, Formal analysis, Investigation. **Guillermo Reyes**: Formal analysis, Investigation. **Orlando J. Rojas**: Funding acquisition, Resources, Writing – review & editing. **Blaise** L. **Tardy**: Conceptualization, Supervision, Writing – original draft, Writing – review & editing. **Erlantz Lizundia**: Supervision, Formal Analysis, Writing – original draft, Writing – review & editing, Funding Acquisition, Resources. All authors have given approval to the final version of the manuscript.

Declaration of competing interest

The authors declare that they have no known competing financial interests or personal relationships that could have appeared to influence the work reported in this paper.

Data availability

Data will be made available on request.

Acknowledgements

The authors acknowledge financial support from the Global Training program of the Basque Government; the "2021 Euskampus Missions 1.0. Programme" granted by Euskampus Fundazioa; the University of the Basque Country (Convocatoria de ayudas a grupos de investigación, GIU21/010); the European Commission Horizon 2020 ERC Advanced program (grant agreement No. 788489 "BioElCell"); the Canada Excellence Research Chair Program (CERC-2018-00006) and the Canada Foundation for Innovation (Project number 38623). BLT is the recipient of the Khalifa University of Science and Technology (KUST) Faculty Startup Project (Project code: 84741140-FSU-2022-021).

Appendix A. Supplementary data

Supplementary data to this article can be found online at https://doi.org/10.1016/j.carbpol.2023.121561.

References

Abbati De Assis, C., Greca, L. G., Ago, M., Balakshin, M. Y., Jameel, H., Gonzalez, R., & Rojas, O. J. (2018). Techno-economic assessment, scalability, and applications of aerosol lignin Micro- and nanoparticles. *ACS Sustainable Chemistry and Engineering, 6*, 11853–11868. https://doi.org/10.1021/acssuschemeng.8b02151

Bai, L., Liu, L., Esquivel, M., Tardy, B. L., Huan, S., Niu, X., … Rojas, O. J. (2022). Nanochitin: Chemistry, structure, assembly, and applications. *Chemical Reviews, 122* (13), 11604–11674. https://doi.org/10.1021/acs.chemrev.2c00125

Berroci, M., Vallejo, C., & Lizundia, E. (2022). Environmental impact assessment of chitin Nanofibril and nanocrystal isolation from Fungi, shrimp shells and crab shells. *ACS Sustainable Chemistry & Engineering, 10*(43), 14280–14293. https://doi.org/10.1021/acssuschemeng.2c04417

Boulos, S., Tännler, A., & Nyström, L. (2020). Nitrogen-to-Protein Conversion Factors for Edible Insects on the Swiss Market: T. molitor, A. domesticus, and L. migratoria. *Frontiers in Nutrition, 7*. https://doi.org/10.3389/fnut.2020.00089

Cabernard, L., Pfister, S., Oberschelp, C., & Hellweg, S. (2022). Growing environmental footprint of plastics driven by coal combustion. *Nature Sustainability, 5*(2), 139–148. https://doi.org/10.1038/s41893-021-00807-2

Chen, C., Wu, Q., Wan, Z., Yang, Q., Xu, Z., Li, D., … Rojas, O. J. (2022). Mildly processed chitin used in one-component drinking straws and single use materials: Strength, biodegradability and recyclability. *Chemical Engineering Journal, 442*, Article 136173. https://doi.org/10.1016/j.cej.2022.136173

Chen, P. Y., Lin, A. Y. M., McKittrick, J., & Meyers, M. A. (2008). Structure and mechanical properties of crab exoskeletons. *Acta Biomaterialia, 4*(3), 587–596. https://doi.org/10.1016/j.actbio.2007.12.010

Cheng, H., Zhao, F., Xue, J., Shi, G., Jiang, L., & Qu, L. (2016). One single graphene oxide film for responsive actuation. *ACS Nano, 10*(10), 9529–9535. https://doi.org/10.1021/acsnano.6b04769

Díaz-Rojas, E. I., Argüelles-Monal, W. M., Higuera-Ciapara, I., Hernández, J., Lizardi-Mendoza, J., & Goycoolea, F. M. (2006). Determination of chitin and protein contents during the isolation of chitin from shrimp waste. *Macromolecular Bioscience, 6*(5), 340–347. https://doi.org/10.1002/mabi.200500233

Dil, E. J., Kim, S. C., Saffar, A., Ajji, A., Zare, R. N., Sattayapiwat, A., … Bowen, R. A. R. (2018). Surface characterization and free thyroid hormones response of chemically modified poly(ethylene terephthalate) blood collection tubes. *Applied Surface Science, 442*, 602–612. https://doi.org/10.1016/j.apsusc.2018.02.177

European Commission. *Climate strategies & targets*. https://climate.ec.europa.eu/eu-action/climate-strategies-targets_en (accessed on July 2023).

Eurostat (2023). Available at https://ec.europa.eu/eurostat/statistics-explained/index.php?title=Recycling_%E2%80%93_secondary_material_price_indicator&oldid=422150 (accessed on September 2023).

Fastmarkets (2023). *US pulp prices tumble for the sixth straight month and drops $60–120 per tonne on oversupply*. https://www.fastmarkets.com/insights/us-pulp-prices-tumble-for-the-sixth-straight-month (accessed on July 2023).

Fazli Wan Nawawi, W. M., Lee, K.-Y., Kontturi, E., Murphy, R. J., & Bismarck, A. (2019). Chitin Nanopaper from mushroom extract: Natural composite of nanofibers and glucan from a single biobased source. *ACS Sustainable Chemistry & Engineering, 7*(7), 6492–6496. https://doi.org/10.1021/acssuschemeng.9b00721

Fischer, W. J., Mayr, M., Spirk, S., Reishofer, D., Jagiello, L. A., Schmiedt, R., … Bauer, W. (2017). Pulp fines—Characterization, sheet formation, and comparison to microfibrillated cellulose. *Polymers, 9*(8), 366. https://doi.org/10.3390/polym9080366

Fu, S. Y., Feng, X. Q., Lauke, B., & Mai, Y. W. (2008). Effects of particle size, particle/matrix interface adhesion and particle loading on mechanical properties of particulate-polymer composites. *Composites Part B: Engineering, 39*(6), 933–961. https://doi.org/10.1016/j.compositesb.2008.01.002

Gómez-Ríos, D., Barrera-Zapata, R., & Ríos-Estepa, R. (2017). Comparison of process technologies for chitosan production from shrimp shell waste: A techno-economic approach using Aspen plus®. *Food and Bioproducts Processing, 103*, 49–57. https://doi.org/10.1016/j.fbp.2017.02.010

Gopalan Nair, K., Dufresne, A., Gandini, A., & Belgacem, M. N. (2003). Crab Shell chitin whiskers reinforced natural rubber nanocomposites. 3. Effect of chemical modification of chitin whiskers. *Biomacromolecules, 4*(6), 1835–1842. https://doi.org/10.1021/bm030058g

Greca, L. G., De France, K. J., Majoinen, J., Kummer, N., Luotonen, O. I. V., Campioni, S., … Tardy, B. L. (2021). Chitin–amyloid synergism and their use as sustainable structural adhesives. *Journal of Materials Chemistry A, 9*(35), 19741–19753. https://doi.org/10.1039/D1TA03215A

Hajiali, F., Vidal, J., Jin, T., de la Garza, L. C., Santos, M., Yang, G., & Moores, A. (2022). Extraction of chitin from green crab shells by Mechanochemistry and aging. *ACS Sustainable Chemistry & Engineering, 10*(34), 11348–11357. https://doi.org/10.1021/acssuschemeng.2c02966

Huang, M., Yang, X., Chen, G., Li, G., & Zhai, P. (2019). Molecular dynamics simulations of the effects of nanopores on mechanical behavior in the Mg2Sn system. *Computational Materials Science, 161*, 177–189. https://doi.org/10.1016/j.commatsci.2019.01.043

Indexbox (2022). Available at https://www.indexbox.io/blog/paper-and-paperboard-price-per-ton-in-august-2022/ (accessed on September 2023).

Inkwood Research (2023), *Global nanocellulose market forecast 2021–2028*. https://inkwoodresearch.com/reports/nano-cellulose-market/#:~:text=The%20price%20of%20cellulose%20nanofibrils,difference%2C%20ultimately%20creating%20economic%20turmoil(accessed on July 2023).

Iturrondobeitia, M., Vallejo, C., Berroci, M., Akizu-Gardoki, O., Minguez, R., & Lizundia, E. (2022). Environmental impact assessment of $LiNi_{1/3}Mn_{1/3}Co_{1/3}O_2$ hydrometallurgical cathode recycling from spent Lithium-ion batteries. *ACS Sustainable Chemistry & Engineering, 10*(30), 9798–9810. https://doi.org/10.1021/acssuschemeng.2c01496

Jin, T., Liu, T., Hajiali, F., Santos, M., Liu, Y., Kurdyla, D., … Moores, A. (2022). High-humidity shaker aging to access chitin and cellulose nanocrystals. *Angewandte Chemie International Edition, 61*(42), Article e202207206. https://doi.org/10.1002/anie.202207206

Jin, T., Liu, T., Lam, E., & Moores, A. (2021). Chitin and chitosan on the nanoscale. *Nanoscale Horizons, 6*(7), 505–542. https://doi.org/10.1039/D0NH00696C

Katakojwala, R., & Mohan, S. V. (2020). Microcrystalline cellulose production from sugarcane bagasse: Sustainable process development and life cycle assessment. *Journal of Cleaner Production, 249*, Article 119342. https://doi.org/10.1016/j.jclepro.2019.119342

Khakalo, A., Filpponen, I., & Rojas, O. J. (2017). Protein adsorption tailors the surface energies and compatibility between Polylactide and cellulose Nanofibrils. *Biomacromolecules, 18*(4), 1426–1433. https://doi.org/10.1021/acs.biomac.7b00173

Khakalo, A., Kouko, J., Filpponen, I., Retulainen, E., & Rojas, O. J. (2017). In-plane compression and biopolymer permeation enable super-stretchable Fiber webs for thermoforming toward 3-D structures. *ACS Sustainable Chemistry & Engineering, 5* (10), 9114–9125. https://doi.org/10.1021/acssuschemeng.7b02025

Khakalo, A., Vishtal, A., Retulainen, E., Filpponen, I., & Rojas, O. J. (2017). Mechanically-induced dimensional extensibility of fibers towards tough fiber networks. *Cellulose, 24*(1), 191–205. https://doi.org/10.1007/s10570-016-1102-z

Kiliona, K. P. S., Zhou, M., Zhu, Y., Lan, P., & Lin, N. (2020). Preparation and surface modification of crab nanochitin for organogels based on thiol-ene click cross-linking. *International Journal of Biological Macromolecules, 150*, 756–764. https://doi.org/10.1016/j.ijbiomac.2020.02.125

Kim, J.-K., Kim, D. H., Joo, S. H., Choi, B., Cha, A., Kim, K. M., … Jin, J. (2017). Hierarchical chitin fibers with aligned Nanofibrillar architectures: A nonwoven-mat separator for Lithium metal batteries. *ACS Nano, 11*(6), 6114–6121. https://doi.org/10.1021/acsnano.7b02085

de Lapuente Díaz de Otazu, R. L., Akizu-Gardoki, O., de Ulibarri, B., Iturriondobeitia, M., Minguez, R., & Lizundia, E. (2021). Ecodesign coupled with life cycle assessment to reduce the environmental impacts of an industrial enzymatic cleaner. *Sustainable Production and Consumption, 29*, 718–729. https://doi.org/10.1016/j.spc.2021.11.016

Larbi, F., García, A., del Valle, L. J., Hamou, A., Puiggalí, J., Belgacem, N., & Bras, J. (2018). Comparison of nanocrystals and nanofibers produced from shrimp shell α-chitin: From energy production to material cytotoxicity and Pickering emulsion properties. *Carbohydrate Polymers, 196*, 385–397. https://doi.org/10.1016/j.carbpol.2018.04.094

Laurent, A., Weidema, B. P., Bare, J., Liao, X., Maia de Souza, D., Pizzol, M., … Verones, F. (2020). Methodological review and detailed guidance for the life cycle interpretation phase. *Journal of Industrial Ecology, 24*(5), 986–1003. https://doi.org/10.1111/jiec.13012

Lebreton, L., & Andrady, A. (2019). Future scenarios of global plastic waste generation and disposal. *Palgrave Communications, 5*(1), 6. https://doi.org/10.1057/s41599-018-0212-7

Li, T., Chen, C., Brozena, A. H., Zhu, J. Y., Xu, L., Driemeier, C., … Hu, L. (2021). Developing fibrillated cellulose as a sustainable technological material. *Nature, 590*, 47–56. https://doi.org/10.1038/s41586-020-03167-7

Liu, M., Peng, Q., Luo, B., & Zhou, C. (2015). The improvement of mechanical performance and water-response of carboxylated SBR by chitin nanocrystals. *European Polymer Journal, 68*, 190–206. https://doi.org/10.1016/j.eurpolymj.2015.04.035

Lizundia, E., Nguyen, T.-D., Winnick, R. J., & MacLachlan, M. J. (2021). Biomimetic photonic materials derived from chitin and chitosan. *Journal of Materials Chemistry C, 9*(3), 796–817. https://doi.org/10.1039/D0TC05381C

Lizundia, E., Ruiz-Rubio, L., Vilas, J. L., & León, L. M. (2016). Towards the development of eco-friendly disposable polymers: ZnO-initiated thermal and hydrolytic degradation in poly(l-lactide)/ZnO nanocomposites. *RSC Advances, 6*, 15660–15669. https://doi.org/10.1039/C5RA24604K

Lu, Y., Cheng, H., Jiang, S., Lin, L., & Lu.. (2023). Impact of three different processing methods on the digestibility and allergenicity of Chinese mitten crab (Eriocheir sinensis) tropomyosin. *Food Science and Human Wellness, 12*, 903–911. https://doi.org/10.1016/j.fshw.2022.09.024

Manavitehrani, I., Fathi, A., Badr, H., Daly, S., Negahi Shirazi, A., & Dehghani, F. (2016). Biomedical applications of biodegradable polyesters. *In Polymers, 8*(1), 20. https://doi.org/10.3390/polym8010020

Mboowa, D. (2021). A review of the traditional pulping methods and the recent improvements in the pulping processes. *Biomass Conversion and Biorefinery*. https://doi.org/10.1007/s13399-020-01243-6

Mushi, E. N., Butchosa, N., Zhou, Q., & Berglund, L. A. (2014). Nanopaper membranes from chitin–protein composite nanofibers—Structure and mechanical properties. *Journal of Applied Polymer Science, 131*(7), 40121. https://doi.org/10.1002/app.40121

Nguyen, H.-L., Ju, S., Hao, L. T., Tran, T. H., Cha, H. G., Cha, Y. J., … Oh, D. X. (2019). The renewable and sustainable conversion of chitin into a chiral nitrogen-doped carbon-sheath nanofiber for enantioselective adsorption. *ChemSusChem, 12*(14), 3236–3242. https://doi.org/10.1002/cssc.201901176

Nguyen, T. D., & Maclachlan, M. J. (2014). Biomimetic chiral Nematic mesoporous materials from crab cuticles. *Advanced Optical Materials, 2*(11), 1031–1037. https://doi.org/10.1002/adom.201400279

Oladipo, H., Yusuf, A., Al-Ali, K., & Palmisano, G. (2021). Techno-economic evaluation of photocatalytic H2S splitting. *Energy Technology, 9*(8), 2100163. https://doi.org/10.1002/ente.202100163

Pelletier, N., Ardente, F., Brandão, M., De Camillis, C., & Pennington, D. (2015). Rationales for and limitations of preferred solutions for multi-functionality problems in LCA: Is increased consistency possible? *The International Journal of Life Cycle Assessment, 20*(1), 74–86. https://doi.org/10.1007/s11367-014-0812-4

Prado, V., Cinelli, M., Ter Haar, S. F., Ravikumar, D., Heijungs, R., Guinée, J., & Seager, T. P. (2020). Sensitivity to weighting in life cycle impact assessment (LCIA). *The International Journal of Life Cycle Assessment, 25*(12), 2393–2406. https://doi.org/10.1007/s11367-019-01718-3

Raabe, D., Romano, P., Sachs, C., Fabritius, H., Al-Sawalmih, A., Yi, S.-B., … Hartwig, H. G. (2006). Microstructure and crystallographic texture of the chitin–protein network in the biological composite material of the exoskeleton of the lobster Homarus americanus. *Materials Science and Engineering: A, 421*(1), 143–153. https://doi.org/10.1016/j.msea.2005.09.115

Razza, N., Castellino, M., & Sangermano, M. (2017). Fabrication of Janus particles via a "photografting-from" method and gold photoreduction. *Journal of Materials Science, 52*(23), 13444–13454. https://doi.org/10.1007/s10853-017-1459-x

Resource recycling (2023). Available at https://resource-recycling.com/recycling/2023/09/11/greif-forecasts-average-48-per-ton-occ-cost-this-year/ (accessed on September 2023).

Rinaudo, M. (2006). Chitin and chitosan: Properties and applications. *Progress in Polymer Science, 31*(7), 603–632. https://doi.org/10.1016/j.progpolymsci.2006.06.001

Rincon-Iglesias, M., Lizundia, E., & Lanceros-Mendez, S. (2019). Water-soluble cellulose derivatives as suitable matrices for multifunctional materials. *Biomacromolecules, 20*(7), 2786–2795. https://doi.org/10.1021/acs.biomac.9b00574

Riofrio, A., Alcivar, T., & Baykara, H. (2021). Environmental and economic viability of chitosan production in Guayas-Ecuador: A robust investment and life cycle analysis. *ACS Omega, 6*(36), 23038–23051. https://doi.org/10.1021/acsomega.1c01672

Roberts, G. A. (2008). Thirty years of progress in chitin and chitosan. *Progress on Chemistry and Application of Chitin and Its Derivatives, 13*, 7–15.

Rødde, R. H., Einbu, A., & Vårum, K. M. (2008). A seasonal study of the chemical composition and chitin quality of shrimp shells obtained from northern shrimp (Pandalus borealis). *Carbohydrate Polymers, 71*, 388–393. https://doi.org/10.1016/j.carbpol.2007.06.006

Rödger, J.-M., Beier, J., Schönemann, M., Schulze, C., Thiede, S., Bey, N., … Hauschild, M. Z. (2021). Combining life cycle assessment and manufacturing system simulation: Evaluating dynamic impacts from renewable energy supply on product-specific environmental footprints. *International Journal of Precision Engineering and Manufacturing-Green Technology, 8*(3), 1007–1026. https://doi.org/10.1007/s40684-020-00229-z

Ruiz, D., Michel, V. M., Niederberger, M., & Lizundia, E. (2023). Chitin Nanofibrils from Fungi for hierarchical gel polymer electrolytes enabling transient zinc ion batteries with stable Zn electrodeposition. *Small, 2303394*. https://doi.org/10.1002/smll.202303394

Sampath, L., Ngasotter, S., Porayil, L., Balange, A. K., Nayak, B. B., Eappen, S., & Xavier, K. A. M. (2022). Impact of extended acid hydrolysis on polymeric, structural and thermal properties of microcrystalline chitin. *Carbohydrate Polymer Technologies and Applications, 4*, Article 100252. https://doi.org/10.1016/j.carpta.2022.100252

Santos, V. P., Marques, N. S. S., Maia, P. C. S. V., Barbosa de Lima, M. A., Franco, L., & Campos-Takaki, G. M. (2020). Seafood waste as attractive source of chitin and chitosan production and their applications. *International Journal of Molecular Sciences, 21*, 4290. https://doi.org/10.3390/ijms21124290

Sarkanen, S., Chen, Y., & Wang, Y.-Y. (2016). Journey to polymeric materials composed exclusively of simple lignin derivatives. *ACS Sustainable Chemistry & Engineering, 4*(10), 5223–5229. https://doi.org/10.1021/acssuschemeng.6b01700

Scaffaro, R., Maio, A., Gulino, F. E., Di Salvo, C., & Arcarisi, A. (2020). Bilayer biodegradable films prepared by co-extrusion film blowing: Mechanical performance, release kinetics of an antimicrobial agent and hydrolytic degradation. *Composites Part A: Applied Science and Manufacturing, 132*, Article 105836. https://doi.org/10.1016/j.compositesa.2020.105836

Seddon, N., Chausson, A., Berry, P., Girardin, C. A. J., Smith, A., & Turner, B. (2020). Understanding the value and limits of nature-based solutions to climate change and other global challenges. *Philosophical Transactions of the Royal Society B: Biological Sciences, 375*(1794), 20190120. https://doi.org/10.1098/rstb.2019.0120

Sehaqui, H., Berglund, L. A., & Zhou, Q. (2013). Biorefinery: Nanofibrillated cellulose for enhancement of strength in high-density paper structures. *Nordic Pulp & Paper Research Journal, 28*(2), 182–189. https://doi.org/10.3183/npprj-2013-28-02-p182-189

Shamshina, J. L., Barber, P. S., Gurau, G., Griggs, C. S., & Rogers, R. D. (2016). Pulping of crustacean waste using ionic liquids: To extract or not to extract. *ACS Sustainable Chemistry & Engineering, 4*(11), 6072–6081. https://doi.org/10.1021/acssuschemeng.6b01434

Strand, A., Sundberg, A., Retulainen, E., Salminen, K., Oksanen, A., Kouko, J., Ketola, A., Khakalo, A., & Rojas, O. (2017). The effect of chemical additives on the strength, stiffness and elongation potential of paper. *Nordic Pulp & Paper Research Journal., 32*(3), 324–335. https://doi.org/10.3183/npprj-2017-32-03-p324-335

Taipale, T., Österberg, M., Nykänen, A., Ruokolainen, J., & Laine, J. (2010). Effect of microfibrillated cellulose and fines on the drainage of Kraft pulp suspension and paper strength. *Cellulose, 17*(5), 1005–1020. https://doi.org/10.1007/s10570-010-9431-9

Tardy, B. L., Mattos, B. D., Otoni, C. G., Beaumont, M., Majoinen, J., Kämäräinen, T., & Rojas, O. J. (2021). Deconstruction and reassembly of renewable polymers and biocolloids into next generation structured materials. *Chemical Reviews, 121*(22), 14088–14188. https://doi.org/10.1021/ACS.CHEMREV.0C01333

Tardy, B. L., Richardson, J. J., Greca, L. G., Guo, J., Bras, J., & Rojas, O. J. (2023). Advancing bio-based materials for sustainable solutions to food packaging. *Nature Sustainability, 6*(4), 360–367. https://doi.org/10.1038/s41893-022-01012-5

Turk, J., Oven, P., Poljanšek, I., Lešek, A., Knez, F., & Malovrh Rebec, K. (2020). Evaluation of an environmental profile comparison for nanocellulose production and supply chain by applying different life cycle assessment methods. *Journal of Cleaner Production, 247*, Article 119107. https://doi.org/10.1016/j.jclepro.2019.119107

Wu, Q., Jungstedt, E., Šoltésová, M., Mushi, N. E., & Berglund, L. A. (2019). High strength nanostructured films based on well-preserved β-chitin nanofibrils. *Nanoscale, 11*(22), 11001–11011. https://doi.org/10.1039/C9NR02870F

Yang, H., Gözaydın, G., Nasaruddin, R. R., Har, J. R. G., Chen, X., Wang, X., & Yan, N. (2019). Toward the Shell biorefinery: Processing crustacean Shell waste using hot water and carbonic acid. *ACS Sustainable Chemistry & Engineering, 7*(5), 5532–5542. https://doi.org/10.1021/acssuschemeng.8b06853

Zimmermann, E. A., Gludovatz, B., Schaible, E., Dave, N. K. N., Yang, W., Meyers, M. A., & Ritchie, R. O. (2013). Mechanical adaptability of the Bouligand-type structure in natural dermal armour. *Nature Communications, 2634*. https://doi.org/10.1038/ncomms3634